Dalton Transactions

RSC Publishing

PAPER

View Article Online
View Journal

Cite this: DOI: 10.1039/c3dt52191e

The first "Kuhn verdazyl" ligand and comparative studies of its $PdCl_2$ complex with analogous 6-oxoverdazyl ligands†

Cooper W. Johnston,[a] Stephen D. J. McKinnon,[a] Brian O. Patrick[b] and Robin G. Hicks*[a]

Received 11th August 2013,
Accepted 21st September 2013

DOI: 10.1039/c3dt52191e

www.rsc.org/dalton

The synthesis and characterization of two new *N*,*N*′-diarylverdazyl radical ligands and their corresponding $PdCl_2$ complexes are described. One of the two radicals is of the "Kuhn verdazyl" structure type and was made by adaptation of standard synthetic procedures for this class of verdazyl. The *N*,*N*′-diphenyl-6-oxoverdazyl was prepared by hydrolysis of a related tetrazane; the resulting *N*,*N*′-diphenylcarbohydrazide was condensed with pyridinecarboxaldehyde and then oxidized to the verdazyl according to standard protocols. Square planar $PdCl_2$ complexes of both verdazyls were prepared by reactions of the radicals with $PdCl_2$ in acetonitrile solution. The structural, spectroscopic, and electrochemical properties of the new verdazyl ligands and their Pd complexes are reported; generally the distinct ligand-centred properties associated with each verdazyl type carry over into the properties of the complexes. The electrochemical studies reveal ligand-centred oxidation and reduction processes; despite the minimal extent of spin delocalization onto Pd in the metal complexes, large shifts in oxidation and reduction potentials (relative to those of the free verdazyl ligands) are discussed.

Introduction

The 'spin-active' and redox-active nature of radical ligands has drawn attention to the magnetic, redox, and chemical reactivity of metal–radical complexes. Radicals such as phenoxyls[1] and nitroxides[2] have a rich coordination chemistry, and complexes of other radical types (*e.g.* thiazyls,[3] aminyls[4,5]) are currently under development. Among the various known classes of stable radicals,[6] verdazyls are notable as the only radical type whose general stability rivals that of the more well-known nitroxides.[7] The coordination chemistry of verdazyls has flourished in the past 15 years, motivated principally by interest in the magnetic properties of metal–verdazyl complexes.[8–13] More recently the redox activity of verdazyls[14] and their metal complexes[15,16] has been revealed, highlighting these radicals as a new entry into the (expanding) redox-active ligand family.

Verdazyl radicals can be subdivided into three broad structure types. All known metal–verdazyl complexes are based on 1,5-dialkyl-6-oxoverdazyls **1** in which the C3 substituent (R′) has a donor site (*e.g.* pyridine, imidazole) which creates a chelating site for metals (*e.g.* **1a**). Coordination complexes of other verdazyl subclasses – 1,5-diaryl-6-oxoverdazyls **2** and 1,3,5-triaryl verdazyls **3** containing a saturated carbon at C6 ("Kuhn" verdazyls, so named here after their discoverer[17]) are as yet unknown. At first glance the structural differences between **1**, **2** and **3** may seem to be relatively minor (particularly between **1** and **2** which differ in the nature (alkyl *vs.* aryl) of the *N*-substituents). However, the physicochemical properties of verdazyl are sensitive to their substituents. For example, whereas most radicals of general structure **1** are orange, 1,5-diaryl-6-oxoverdazyls **2** are deep red and 1,3,5-triaryl verdazyls **3** are green. The redox properties of each verdazyl type are also distinctive;[14] the oxidation and reduction potentials of **1–3** both span a potential range of over 0.5 V. Derivatives of **3** are generally the easiest to oxidize and hardest to reduce and derivatives of **2** are relatively difficult to oxidize and easy to reduce. The chemical properties of different verdazyl types are also distinct from one another. For example, whereas derivatives of **1** can be used in controlling radical polymerization,[18] Kuhn verdazyls **3** are ineffective.[19] We became interested in exploring how the differences in steric profiles and physicochemical properties of verdazyls of type **1–3** would be expressed in their respective coordination complexes. In particular the coordination chemistry of Kuhn verdazyls **3** in which the tetrazine

[a]*Department of Chemistry, University of Victoria, PO Box 3065 STN CSC, Victoria, BC V8W 3V6, Canada. E-mail: rhicks@uvic.ca*
[b]*Crystallography Laboratory, Department of Chemistry, University of British Columbia, Vancouver, BC V6 T 1Z1, Canada*

†Electronic supplementary information (ESI) available: Crystallographic data (cif format) for **2a**, **2a**·$PdCl_2$ and **3a**·$PdCl_2$. CCDC 943810–943812. For ESI and crystallographic data in CIF or other electronic format see DOI: 10.1039/c3dt52191e

heterocycle is directly bound to a metal are unknown, although "spin labelled" complexes in which Kuhn verdazyls are remotely attached to a ligand have been reported.[20] Herein we report the first transition metal complexes of 1,5-diaryl-6-oxoverdazyl **2a** and Kuhn verdazyl **3a** and compare the properties of these complexes with those of the analogous 1,5-dialkyl-6-oxoverdazyl ligand **1a**.[10]

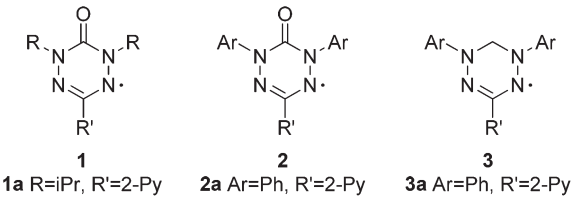

Results and discussion

Ligand and complex synthesis

Ligand **1a**[9] and its $PdCl_2$ complex[10] were made as previously reported. Kuhn verdazyl **3a** was made by adaptation of established protocols for the synthesis of this class of verdazyl (Scheme 1); thus, reaction of formazan **4** with formaldehyde under basic conditions yielded radical **3a** as a grass-green solid which is very acid-sensitive (Kuhn verdazyls are prone to acid-induced disproportionation).[7] This sensitivity may contribute to our inability to obtain adequate microanalytical data for this radical. Reaction of **3a** with $PdCl_2$ in hot acetonitrile gave **3a**·$PdCl_2$ as a dark green crystalline solid.

The precursor to desired verdazyl **2a**, *i.e.* tetrazane **7**, could not be made using the conventional Milcent-based procedure (*i.e.*, careful reaction of phosgene with a hydrazine, followed by treatment of the chloroformylhydrazone intermediate with a monosubstituted hydrazine[21,22]). We then targeted *N*,*N*′-diphenyl carbohydrazide **6** as a precursor to tetrazane **7**, by analogy to the conventional syntheses of *N*,*N*′-dialkyl 6-oxotetrazanes.[7,23] A recent report claimed that desired *N*,*N*′-diphenyl carbohydrazide **6** could be made by metal-catalyzed bis-arylation of carbohydrazide ($H_2NNHC(O)NHNH_2$),[24] but these results could not be reproduced in our hands. We were able to make carbohydrazide **6** by hydrolysis of tetrazane **5**[22] (Scheme 2). Subsequent condensation of **6** with 2-pyridinecarboxaldehyde gave tetrazane **7** which was then oxidized with silver oxide/celite to afforded the desired radical as a dark red compound. The $PdCl_2$ complex of this radical was made using the same procedures as for **3a**·$PdCl_2$.

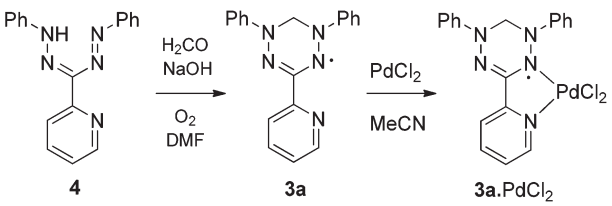

Scheme 1 Synthesis of Kuhn verdazyl **3a** and its $PdCl_2$ complex.

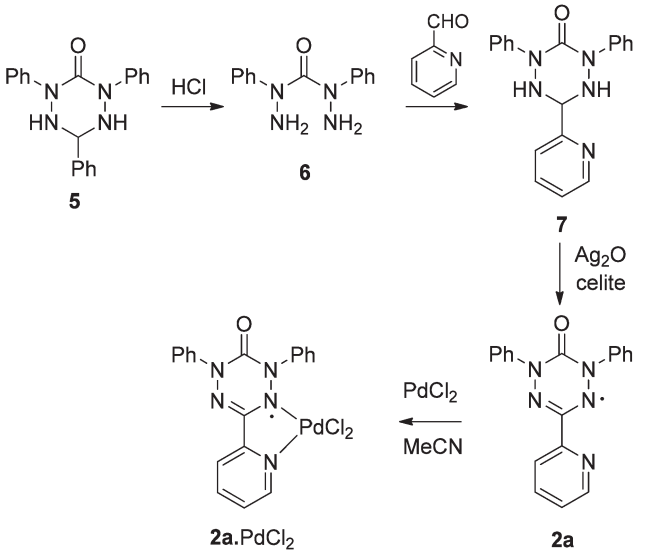

Scheme 2 Synthesis of *N*,*N*′-diphenyl-6-oxoverdazyl **2a** and its corresponding $PdCl_2$ complex.

X-ray structures

The structures of ligand **1a**[9] and its $PdCl_2$ complex[10] has been reported. We have been able to obtain X-ray quality crystals of ligand **2a**, but not **3a**. The structure of **2a** is shown in Fig. 1. Bond parameters within the tetrazine ring are typical for 1,5-diaryl-6-oxoverdazyls.[21,24,25] Torsion angles of the aromatic substituents with respect to the tetrazine ring are 36.3° (for the *N*-phenyl ring attached to N2), 33.1° (*N*-phenyl ring N3) and 8.1° (for the 2-pyridyl attached to C2).

The structures of **2a**·$PdCl_2$ and **3a**·$PdCl_2$ are presented in Fig. 2 and 3 respectively; selected bond lengths for these complexes, along with those of **1a**·$PdCl_2$ (provided for comparative purposes) are found in Table 1. All three complexes consist of a square-planar Pd(II) ion chelated by a verdazyl radical in the *N*,*N*′-bidentate mode. It is worth noting that the pendant *N*-phenyl groups do *not* cyclometallate in either case. This contrasts the norm in square planar Pd(II) complexes containing bipyridine ligands with *ortho*-phenyl substituents, in which the ligand adopts an NNC tridentate binding mode *i.e.*, **8**.[26]

Fig. 1 Structure of **2a**. Hydrogen atoms removed for clarity. Thermal ellipsoids drawn at 50% probability. Selected bond lengths (Å) C1–O1 1.225(5); C1–N2 1.363(5); C1–N3 1.389(5); C2–N4 1.333(5); C2–N1 1.337(5); C2–C15 1.477(5); N1–N2 1.369(5); N3–N4; 1.376(5).

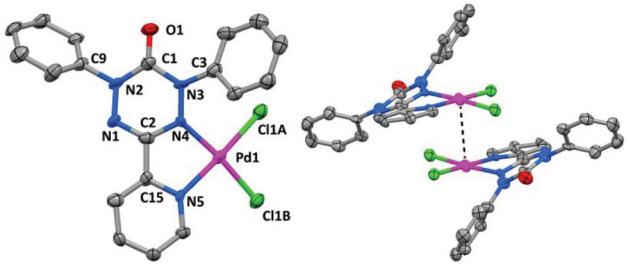

Fig. 2 Structure of **2a**·$PdCl_2$. Left: partial atom labelling scheme. Right: perpendicular view showing Pd–Pd interaction. Hydrogen atoms removed for clarity. Thermal ellipsoids drawn at 50% probability.

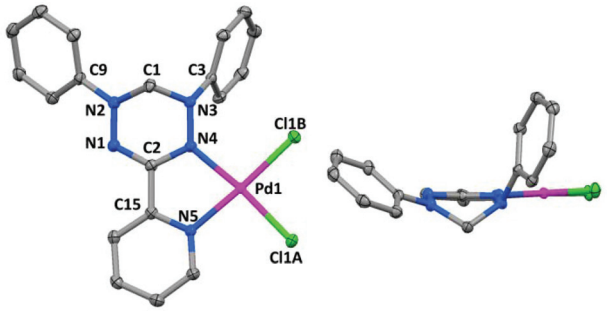

Fig. 3 Structure of **3a**·$PdCl_2$. Left: partial atom labeling scheme. Right: perpendicular view. Hydrogen atoms removed for clarity. Thermal ellipsoids drawn at 50% probability.

Table 1 Selected bond lengths for Pd–verdazyl complexes

Bond	**1a**·$PdCl_2$ [10]	**2a**·$PdCl_2$	**3a**·$PdCl_2$
Pd1–N4	2.064(2)	2.064(7)	2.0253(12)
Pd1–N5	2.029(2)	2.076(7)	2.0310(13)
N3–N4	1.374(3)	1.348(10)	1.3813(17)
N1–N2	1.353(3)	1.358(11)	1.3353(18)
C2–N1	1.313(3)	1.322(13)	1.3361(19)
C2–N4	1.341(4)	1.371(12)	1.3413(19)
C1–O1	1.211(4)	1.220(12)	—

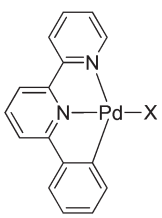

8

The bond metrics within the verdazyl ring of the complexes are broadly comparable (Table 3); all three complexes show desymmetrization of the C2–N1/C2–N4 bonds in the ligand to varying degrees, with the CN bond adjacent to Pd being slightly longer than the remote CN bond. There are also small perturbations in the NN bonds in all cases, but all fall within ranges seen for other metal–verdazyl complexes. **2a**·$PdCl_2$ adopts a dimeric structure in the solid state *via* weak Pd–Pd contacts in the solid state (Fig. 2), whereas **3a**·$PdCl_2$ (and **1a**·$PdCl_2$) do not, although $PdCl_2$ complexes of other derivatives of **1** do adopt this dimeric motif. The presence/absence of weak Pd–Pd interactions is presumably influenced by intermolecular packing effects.

The effect of the *N*3-phenyl substituent on the structures of the complexes of **2a** and **3a** is substantial. In **1a**·$PdCl_2$ the *N*-isopropyl group adjacent to the palladium ion adopts an orientation to minimize its steric interactions with $PdCl_2$ unit, which results in ligand **1a** possessing an essentially planar conformation as bound to Pd.[10] For **2a**·$PdCl_2$ the *N*-phenyl group forces a slight torsion of the tetrazine ring relative to the pyridine (18.2°) but the trivalent nitrogen (N3) remains essentially planar (sum of angles = 359.3°). In **3a**·$PdCl_2$ the tetrazine and pyridine rings remain coplanar, but the geometry at N3 is modestly pyramidalized (349°) (the remote trivalent nitrogen, N2, is trigonal planar (359.9°)). As a result the N3–C(Ph) bond is tilted by 59.8° with respect to the plane defined by the conjugated (N2–N1–C2–N3–N3) subunit of the tetrazine ring. The displacement of the saturated carbon C1 from this plane is a normal structural feature of Kuhn verdazyls.[7]

EPR spectroscopy

We previously reported the solution EPR spectra of ligand **1a** and its $PdCl_2$ complex.[10] The spectra of **2a** and **2a**·$PdCl_2$ are presented in Fig. 4, while the spectra of **3a** and **3a**·$PdCl_2$ are shown in Fig. 5. Spectral data for all ligands and complexes are compiled in Table 2. The hyperfine coupling constants (obtained from spectral simulation) for the two ligands **2a** and **3a** are representative of each verdazyl structure type. The spin distribution is found predominantly on the four tetrazine nitrogen atoms. Previous EPR/ENDOR studies on related diaryl verdazyls have identified small but non-negligible spin density on the *N*-phenyl substituents,[21,27] but the magnitude of the coupling to the aromatic protons is too small to be observed in the present compounds.

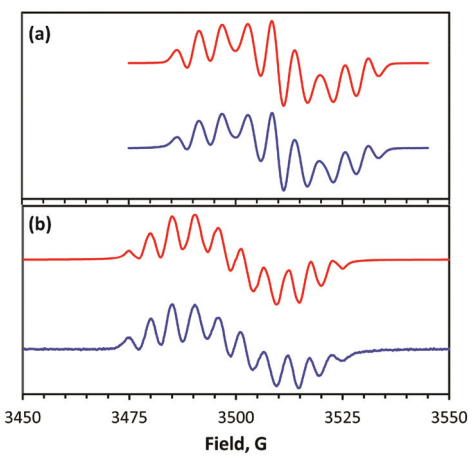

Fig. 4 (a) Experimental (blue) and simulated (red) EPR spectra of **2a** in CH_2Cl_2 solution at room temperature. (b) Experimental (blue) and simulated (red) EPR spectra of **2a**·$PdCl_2$ in CH_2Cl_2 solution at room temperature. Microwave frequencies for **2a** and **2a**·$PdCl_2$ are 9.8457 and 9.8462 GHz, respectively.

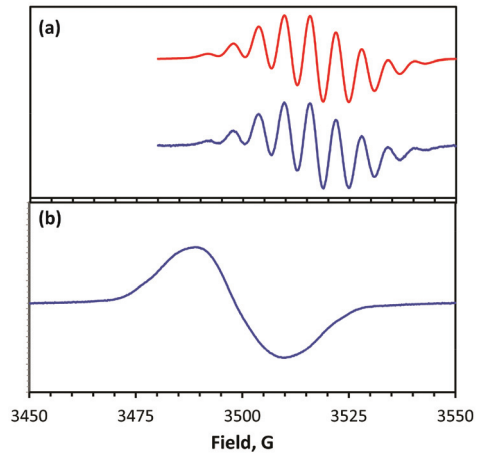

Fig. 5 (a) Experimental (blue) and simulated (red) EPR spectra of **3a** in CH_2Cl_2 solution at room temperature. (b) Experimental spectra of **3a**·$PdCl_2$ in CH_2Cl_2 solution. Microwave frequencies for **3a** and **3a**·$PdCl_2$ are 9.8464 and 9.8470 GHz, respectively.

Table 2 EPR parameters

	2a	**2a**·$PdCl_2$	**3a**	**3a**·$PdCl_2$
g	2.0028	2.0087	2.0042	2.0120
a(N)	4.57	4.74	5.78	—
a(N)	4.57	4.79	5.78	—
a(N)	6.49	5.76	5.87	—
a(N)	6.49	8.04	5.87	—

The EPR spectra of the Pd complexes of **2a** and **3a** show the expected shift in g-value which arises from spin density on the palladium nucleus (see below). The g-values of the complexes are similar to those of other verdazyl–Pd complexes.[10] Consistent with the EPR spectra of verdazyl complexes of other metal ions,[12] metal ion coordination causes modest changes in the spin distribution in the tetrazine ring of the verdazyl for **2a**·$PdCl_2$. As we found previously for other Pd–verdazyl complexes,[10] any coupling to the palladium nucleus (^{105}Pd (22.3% abundance), I = 5/2) is too small to be observed in the spectrum of **2a**·$PdCl_2$. Unfortunately, no fine structure is evident at all in the spectrum of **3a**·$PdCl_2$, precluding detailed analysis. However the magnitudes of the shift in g-value of all three Pd complexes are similar, suggesting similar (small) magnitudes of spin density on the Pd ion for each case.

Electronic spectroscopy

The UV-visible spectra of ligands **1a**, **2a**, and **3a** are presented in Fig. 6. The spectra of the three ligands have distinct low-energy absorption maxima (410, 518, and 693 nm, respectively) which are characteristic of each verdazyl type (**1**, **2** or **3**). The significant spectral differences between **1a** and **2a** clearly implicate the involvement of the *N*-aryl groups (the only structural difference between **2a** and **1a**) in the lowest energy transitions. The UV-visible spectra of the three Pd complexes are shown in Fig. 7. The lowest energy transitions in the electronic

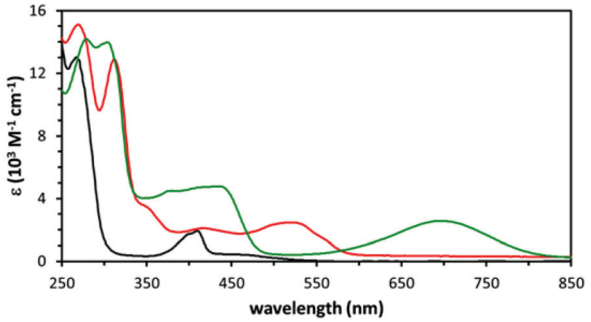

Fig. 6 Electronic spectra of **1a** (black line), **2a** (red line), and **3a** (green line) in MeCN.

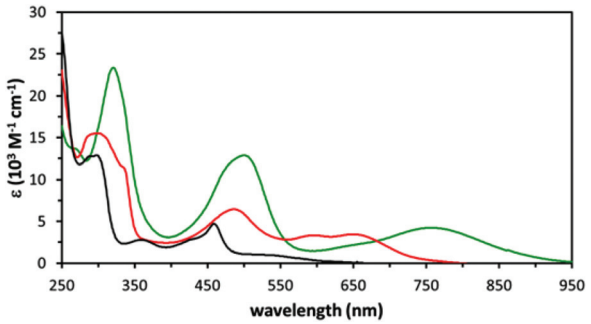

Fig. 7 Electronic spectra of **1a**·$PdCl_2$ (black line), **2a**·$PdCl_2$ (red line), and **3a**·$PdCl_2$ (green line). Spectra recorded in CH_2Cl_2 solution.

spectra of the $PdCl_2$ complexes of **1a** and **3a** are, to a good approximation, red-shifted from the spectra of the corresponding free ligand. However the spectrum of **2a**·$PdCl_2$ consists of a multiple absorption bands between 600–700 nm, some of which may be charge-transfer in nature.

Electrochemistry

The cyclic voltammograms of ligands **1a**, **2a**, and **3a** and their corresponding $PdCl_2$ complexes are presented in Fig. 8: pertinent electrochemical parameters are compiled in Table 3. The voltammograms of all three ligands contain reversible oxidation and reduction processes. The oxidation and reduction potentials for each fall within the normal range for the *general* verdazyl structure type (**1**, **2**, or **3**) of which they are representatives. Thus, the Kuhn verdazyl **3a** is considerably easier to oxidize and harder to reduce than the two oxoverdazyls **1a** and **2a** which we have previously rationalized as arising from the electron-withdrawing carbonyl groups in the latter two.[14] The *difference* between oxidation and reduction potentials of a given radical – known as its *cell potential*, E_{cell} [28,29] – have also been previously discussed[14] for general derivatives of **1**, **2**, and **3**: qualitatively the values of E_{cell} correlate with the degree of delocalization. The two *N*,*N*′-diaryl verdazyls (**2a** and **3a**), in which spin delocalization onto the *N*-aryl rings is evident, have somewhat smaller E_{cell} values than that of **1a** (Table 3), which does not have *N*-aryl substituents. The differences between **2a**

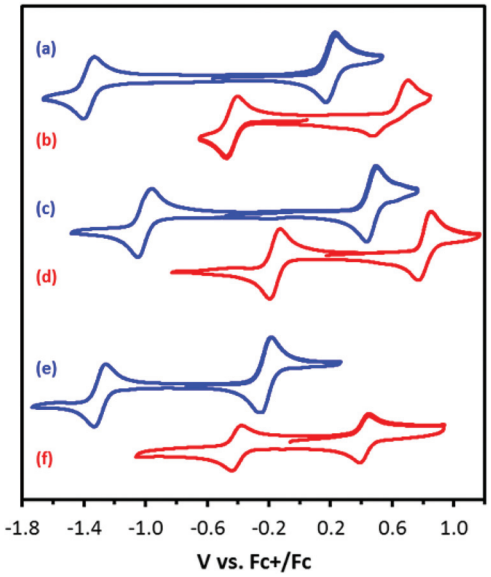

Fig. 8 Cyclic voltammograms of (a) **1a**, (b) **1a**·$PdCl_2$ (c) **2a**, (d) **2a**·$PdCl_2$, (e) **3a**, (f) **3a**·$PdCl_2$. 1 mM analyte, 0.1 M Bu_4NBF_4 electrolyte, CH_2Cl_2 solutions, scan rate 100 mV s^{-1}.

Table 3 Electrochemical data. Potentials are in V *vs.* Fc^+/Fc in CH_2Cl_2 solution

Cpd	E°_{red}	E°_{rox}	E_{cell}
1a	−1.37	+0.20	1.57
1a·$PdCl_2$	−0.44	+0.67[a]	1.11[b]
2a	−1.00	+0.47	1.47
2a·$PdCl_2$	−0.16	+0.81	0.97
3a	−1.30	−0.22	1.08
3a·$PdCl_2$	−0.41	+0.42	0.83

[a] Irreversible process; anodic peak potential given. [b] E_{cell} calculated using anodic peak potential.

and **3a** are consistent with the larger degree of *N*-aryl substituent spin delocalization.[21]

The voltammograms of each of the $PdCl_2$ complexes also consist of a ligand-centred oxidation and reduction. All such processes are reversible except for the oxidation of **1a**·$PdCl_2$ (Fig. 8). Each redox process for a given complex is shifted to more positive potential relative to the corresponding process for the free ligand. In other words, all of the verdazyl radicals become easier to reduce and harder to oxidize upon coordination to Pd(II). We have noted similar behaviour in Zn(II) verdazyl complexes.[16] One noteworthy feature of the voltammograms of the Pd complexes is that, for each of the verdazyls, the magnitude of the shift of the reduction potential upon coordination is substantially larger than the shift of the oxidation potential. The verdazyl reduction potentials shift by 0.84–0.93 V, while the shift in oxidation potentials is smaller and more variable (0.34–0.64 V). A consequence of this observation is that the E_{cell} values for the complexes are significantly smaller than the values of the free ligands (Table 3). As discussed above, arguments have been put forth correlating E_{cell} with the extent of delocalization (basically, the size/space of the conjugated framework encompassing spin density) of an organic radical.[29] The spectroscopic data for the Pd complexes presented herein suggest minimal spin delocalization onto the Pd ion, yet the complexes have much smaller E_{cell} values than the free ligands. The origin of the effect of the Pd ion on the verdazyl ligand's redox properties may, therefore, be inductive in nature – an effect with differing magnitude of consequences for the reduction and oxidation processes of the verdazyl.

Conclusions

Herein we have presented two new verdazyl radical ligands, thereby expanding the toolkit of verdazyl coordination chemistry, including the first Kuhn verdazyl capable of binding directly to transition metals. The distinctive spectroscopic and particularly the redox properties associated with each ligand type carry over into their respective Pd complexes. The ligand-centred redox events in the metal complexes cannot be rationalized based on delocalization arguments and point to an inductive "metal-as-substituent" effect which will require a larger array of complexes to better understand.

Experimental section

General considerations

All solvents and reagents were purchased from Aldrich and used as received without further purification unless otherwise stated. 1,3,5-Triphenyl 6-oxotetrazane[22] and 2-pyridinecarboxaldehyde phenylhydrazone[30] were synthesized using literature methods.

^1H and ^{13}C NMR spectra were recorded on a Bruker AC300 (300 MHz) instrument. FT-IR spectra were recorded on a Perkin-Elmer Spectrum One FT-IR spectrometer as pressed KBr discs. EPR spectra were recorded on a Bruker EMX instrument (9.85 GHz) with samples prepared as dilute (~10^{-4} M) and deoxygenated (purging with Ar) solutions. A DPPH radical standard (g = 2.0036) was used as a field reference. The EPR spectra were simulated using the WinSim 2002 program. UV-Vis spectra were recorded on a Perkin-Elmer Lambda 1050 spectrometer. Melting points were determined using a Gallenkamp melting point apparatus and are uncorrected. Elemental analyses were performed by Canadian Microanalytical Services Ltd, Delta, British Columbia, Canada. CV experiments were performed using a Bioanalytical Systems E2 Epsilon Electrochemical Analyzer with a cell consisting of a glassy carbon working electrode, platinum wire counter electrode, and a silver wire reference electrode. Crystallographic data are summarized in Table 4.

1,5-Diphenyl-3-(2-pyridyl)formazan (4). 2-Pyridinecarboxaldehyde phenylhydrazone (2.19 g, 11.1 mmol) was added to a mixture of EtOH (10 mL), H_2O (70 mL), and CH_2Cl_2 (120 mL). The solution was cooled to −5 °C and $Na_2CO_3·H_2O$ (5.57 g, 44.9 mmol) and $n$$Bu_4NBr$ (0.44 g, 1.4 mmol) were added.

Table 4 Crystallographic data

	2a	**2a**·$PdCl_2$	**3a**·$PdCl_2$
Empirical formula	$C_{19}H_{14}N_5O$	$C_{19}H_{14}N_5OPdCl_2$	$C_{19}H_{16}N_5PdCl_2$
Formula wt	328.35	505.65	491.67
T (K)	90	90	90
Wavelength (Å)	0.71073	0.71073	0.71073
Crystal system	Orthorhombic	Triclinic	Monoclinic
Space group	$Pna2_1$ (#33)	$P\bar{1}$ (#2)	$P2_1/c$ (#14)
a (Å)	11.2176(4)	9.421(1)	8.4974(8)
b (Å)	19.5159(6)	10.034(1)	14.1240(13)
c (Å)	7.0585(2)	11.028(1)	15.4290(15)
α (°)	90	77.160(7)	90
β (°)	90	77.700(6)	99.586(5)
γ (°)	90	72.661(6)	90
V (Å^3)	1545.26(8)	958.1(2)	1825.8(3)
Z	4	2	4
μ (cm^{-1})	0.93	12.68	13.24
ρ_{calc} (g cm^{-3})	1.411	1.753	1.789
Data collected	18 023	9294	31 632
Unique data	2837	2439	5304
Parameters	226	253	244
g.o.f.	1.13	1.20	1.09
R_1	0.073	0.088	0.023
wR_2 (all data)	0.202	0.156	0.050
CCDC#	943810	943811	943812

A solution of benzenediazonium chloride (made by mixing H_2O (10 mL), aniline (1.20 mL, 13.0 mmol), and 37% HCl (4 mL, 46.6 mmol) followed by cooling to −5 °C; a solution of $NaNO_2$ (1.04 g, 15.1 mmol) at −5 °C was added dropwise to it and the resulting solution was allowed to stir for 30 minutes) was added dropwise to the biphasic solution producing an gradual colour change from yellow to blood red. The solution was stirred for 1 h at −5 °C. The solution added to a separatory funnel and CH_2Cl_2 (100 mL) was added to the funnel. The organic layer was washed with H_2O (5 × 100 mL) and stored on $MgSO_4$. The solvent was removed *in vacuo* and the deep red residue was purified by column chromatography on alumina (hexanes–CH_2Cl_2, 8 : 2) followed by a second column on silica (hexanes–CH_2Cl_2–EtOAc, 7 : 2 : 1). The product was taken up in EtOAc and the solvent was removed *in vacuo*, this was repeated until a dark red solid was obtained (1.30 g, 39.0%). ^{1}H NMR (300 MHz, CD_2Cl_2): δ 15.61 (s, 1H, NH), 14.25 (s, 1H, NH), 8.76 (ddd, 1H, J = 5, 2, 1 Hz), 8.71 (ddd, 1H, J = 5, 2, 1 Hz), 8.27 (dt, 1H, J = 8, 1 Hz), 8.14 (dt, 1H, J = 8, 1 Hz), 7.95 (dd, 2H, J = 8, 2 Hz), 7.91 (td, 1H, J = 8, 2 Hz), 7.79 (td, 1H, J = 8, 2 Hz), 7.74 (dd, 4H, J = 8, 2 Hz), 7.35 (m, 15H), 7.04 (tt, 1H, J = 7, 2 Hz) ppm. ^{13}C NMR (300 MHz, CD_2Cl_2): δ 155.5, 153.8, 153.0, 149.7, 148.1, 147.5, 144.0, 143.3, 141.9, 137.3, 136.7, 129.9, 129.8, 129.5, 128.2, 124.1, 123.3, 123.2, 122.9, 122.7, 121.7, 119.3, 115.3 ppm. FT-IR (KBr): 3369 (w), 3049 (m), 1599 (m), 1584 (s), 1565 (m), 1501 (s), 1470 (s), 1450 (s), 1430 (s), 1351 (s), 1240 (s), 1076 (s), 1058 (s), 1036 (s), 994 (m), 926 (w), 894 (w), 792 (m), 767 (m), 754 (s), 741 (s), 696 (m), 685 (s), 653 (m), 633 (m), 588 (m), 546 (w), 501 (w) cm^{-1}. UV-Vis (CH_2Cl_2): λ_{max} (nm) (ε, M^{-1} cm^{-1}) 262 (1.4 × 10^4), 308 (1.9 × 10^4), 464 (1.9 × 10^4). MS (ESI): m/z LR-MS 324 (M + Na$^+$, 100%), HR-MS: theor 302.14057 (M+H)$^+$, expt 302.13969 (M + H$^+$, 100%). MP: 106–109 °C.

1,5-Diphenyl-3-(pyridin-2-yl)verdazyl (3a). To 1,5-diphenyl-3-(pyridin-2-yl)formazan **4** (522 mg, 1.73 mmol) was added DMF (25 mL). A 37% solution of formaldehyde (1.9 mL, 26 mmol) was added and the resulting solution was left to stir for 1 h. A solution of 2 M NaOH (5.5 mL, 11 mmol) was added dropwise. The solution was allowed to stir at RT and open to air for 23 h. It was poured into Et_2O (200 mL), washed with H_2O (5 × 50 mL), and the organic layer was stored on Na_2CO_3. The solvent was removed *in vacuo* and the dark residue was chromatographed on deactivated neutral alumina (hexanes–CH_2Cl_2–NEt_3, 14 : 6 : 1) yielding **3a** as a dark green solid (81.5 mg, 15.0%). FT-IR (KBr): 3057 (w), 2957 (w), 1685 (w), 1588 (s), 1567 (m), 1495 (s), 1476 (s), 1457 (m), 1393 (m), 1368 (m), 1314 (m), 1304 (m), 1270 (m), 1216 (w), 1147 (m), 1130 (m), 1076 (w), 1028 (w), 994 (w), 940 (w), 894 (w), 789 (m), 748 (s), 687 (m), 650 (w), 628 (w), 622 (w), 612 (w), 603 (m) cm^{-1}. UV-Vis (MeCN): λ_{max} (nm) (ε, M^{-1} cm^{-1}), 279 (1.4 × 10^4), 304 (1.4 × 10^4), 380 (4.5 × 10^3), 435 (4.8 × 10^3), 693 (2.6 × 10^3). MS (ESI): m/z LR-MS 315 (M + H$^+$, 100%), HR-MS: theor 314.14057 (M$^+$), expt 314.13997 (M$^+$, 100%). Anal. Calc. for $C_{19}H_{16}N_5$: C, 72.59; H, 5.13; N, 22.28. Found: C, 72.47; H, 5.08; N, 20.87. MP: 80–84 °C.

[1,5-Diphenyl-3-(pyridin-2-yl)verdazyl]palladium(II) chloride (3a·$PdCl_2$). $PdCl_2$·$2H_2O$ (37.4 mg, 0.175 mmol) was added to MeCN (20 mL) and the solution was heated to reflux. A solution of **3a** (59.4 mg, 0.189 mmol) in MeCN (5 mL) was added dropwise. The resulting solution was stirred for 15 min at reflux. The solution was cooled and left to stand. A dark green crystalline solid was collected by filtration (42 mg, 48%). FT-IR (KBr): 3466 (br, m), 3047 (s), 2920 (w), 1607 (m), 1584 (m), 1487 (s), 1458 (s), 1424 (s), 1392 (m), 1344 (m), 1288 (m), 1266 (m), 1243 (m), 1199 (m), 1161 (m), 1146 (m), 1136 (m), 1108 (m), 1100 (m), 1077 (w), 1050 (w), 1035 (w), 1027 (w), 1003 (w), 969 (w), 951 (m), 906 (w), 766 (s), 755 (s), 700 (m), 680 (m), 655 (m), 629 (m), 602 (w), 575 (w), 535 (w) cm^{-1}. UV-Vis (MeCN): λ_{max} (nm) (ε, M^{-1} cm^{-1}) 314 (9.8 × 10^3), 489 (5.3 × 10^3), 733 (1.7 × 10^3). Anal. Calc. for $C_{19}H_{16}N_5PdCl_2$: C, 46.41; H, 3.28; N, 14.24. Found: C, 46.35; H, 3.15; N, 14.32. MP: 202–208 °C.

2,4-Diphenylcarbonohydrazide (6). 2,4,6-Triphenyl tetrazane **5** (2.480 g, 7.507 mmol) was combined with 80 mL of 37% HCl and 30 mL H_2O. The solution was stirred for 24 h and then refluxed for 2 h. After cooling, the solution was added to a separatory funnel and was washed with CH_2Cl_2 (3 × 50 mL). CH_2Cl_2 (60 mL) was added to the funnel and the solution was rendered basic using 2 M NaOH until pH 14 was reached. The aqueous phase was then extracted with CH_2Cl_2 (4 × 60 mL) and the organic layer was dried using $MgSO_4$. The solvent was removed *in vacuo* leaving a yellow oil which solidified. The yellowish solid was collected (1.375 g, 75.6%). ^{1}H NMR (300 MHz, DMSO-d_6): δ 7.29 (dd, 4H, J = 8, 1 Hz), 7.20 (t, 4H, J = 7 Hz), 6.95 (2H, tt, J = 7, 1 Hz), 5.24 (4H, s) ppm. ^{13}C NMR (300 MHz, DMSO-d_6): δ 160.8, 145.5, 127.9, 123.0, 121.5 ppm. FT-IR (KBr): 3342 (s), 3313 (s), 3282 (s), 3063 (m), 3039 (m), 1653 (s), 1620 (s), 1585 (s), 1494 (s), 1363 (s), 1305 (s), 1179 (m), 1091 (m), 1076 (m), 1024 (m), 921 (s), 901 (s), 775 (s), 766 (s), 748 (s),

693 (s), 658 (m), 603 (m), 536 (m) cm^{-1}. UV-Vis (MeCN): λ_{max} (ε, M^{-1} cm^{-1}) 266 (1.2×10^4). MS (ESI): *m*/*z* LR-MS 265 (M + Na^+, 100%), HR-MS: theor 243.12459 ($M+H^+$), expt 243.12385 (M + H^+, 100%). Anal. Calc. for $C_{13}H_{14}N_4O$: C, 64.45; H, 5.82; N, 23.13. Found: C, 64.47; H, 5.65; N, 23.22. MP: 74–77 °C.

2,4-Diphenyl-6-(pyridin-2-yl)-1,2,4,5-tetrazinan-3-one (7). To MeOH (15 mL) was added **6** (317 mg, 1.31 mmol), 2-pyridinecarboxaldehyde (0.11 mL, 1.2 mmol) followed by pyridinium tosylate (108 mg, 0.430 mmol). The bright yellow solution was stirred at room temperature for 48 h. It was then poured into H_2O (90 mL) and stirred for 3 h to form a white precipitate which was collected by filtration. The product was washed with H_2O and dried overnight to yield a white solid (371 mg, 94.7%). ^1H NMR (300 MHz, DMSO-d_6): δ 8.56 (ddd, 1H, J = 5, 2, 1 Hz), 7.84 (td, 1H, J = 8, 2 Hz), 7.64–7.53 (mult, 5H), 7.39 (ddd, 1H, J = 8, 5, 1 Hz), 7.30 (tt, 4H, J = 8, 2 Hz), 7.05 (tt, 2H, J = 7, 1 Hz), 6.49 (d, 2H, J = 10 Hz), 5.40 (t, 1H, J = 10 Hz) ppm. ^{13}C NMR (300 MHz, DMSO-d_6): δ 156.8, 156.3, 148.7, 142.8, 137.2, 128.0, 123.8, 123.3, 122.7, 121.1, 73.4 ppm. FT-IR (KBr): 3222 (m), 3066 (w), 3029 (w), 1653 (s), 1596 (s), 1570 (w), 1484 (s), 1455 (m), 1440 (m), 1360 (s), 1299 (s), 1111 (w), 1090 (w), 1031 (w), 997 (m), 898 (s), 796 (m), 751 (s), 706 (m), 693 (s), 647 (w), 593 (w), 568 (m) cm^{-1}. UV-Vis (MeCN): λ_{max} (ε, M^{-1} cm^{-1}) 263 (2.3×10^4). MS (ESI): *m*/*z* LR-MS 354 (M + Na^+, 100%), HR-MS: theor 332.15114 $(M+H)^+$, expt 332.15031 (M + H^+, 100%). Anal. Calc. for $C_{19}H_{17}N_5O$: C, 68.87; H, 5.17; N, 21.13. Found: C, 69.28; H, 4.99; N, 21.25. MP: 143–147 °C.

1,5-Diphenyl-3-(pyridin-2-yl)6-oxoverdazyl (2a). To MeOH (5 mL) was added **7** (97.0 mg, 0.293 mmol), celite (92.0 mg), and silver oxide (102 mg, 0.439 mmol). The resulting solution was stirred for 1 h. The solvent was removed in vacuo and the residue was purified by chromatography using silica gel (hexanes-EtOAc-CH_2Cl_2, 2:1:1) and the major red fraction was collected (56 mg, 58%). FT-IR (KBr): 3089 (w), 3065 (w), 3013 (w), 1743 (w), 1696 (s), 1589 (m), 1570 (m), 1485 (s), 1457 (m), 1401 (m), 1368 (m), 1298 (m), 1258 (m), 1238 (m), 1136 (m), 1125 (m), 994 (w), 1088 (w), 1044 (w), 1024 (w), 897 (w), 798 (w), 758 (s), 713 (w), 692 (s), 654 (m), 631 (m), 619 (m), 612 (m), 601 (s) cm^{-1}. UV-Vis (MeCN): λ_{max} (nm) (ε, M^{-1} cm^{-1}): 269 (1.5×10^4), 312 (1.3×10^4), 416 (2.1×10^3), 518 (2.5×10^3). MS (ESI): *m*/*z* LR-MS 351 (M + Na^+, 100%), HR-MS: theor 329.12766 ($M+H^+$), expt 329.12661 (M + H^+, 100%). Anal. Calc. for $C_{19}H_{14}N_5O$: C, 69.50; H, 4.30; N, 21.33. Found: C, 69.43; H, 4.16; N, 21.37. MP: 206–209 °C.

[1,5-Diphenyl-3-(pyridin-2-yl)6-oxoverdazyl]palladium(II) chloride (2a·PdCl$_2$). Solid $PdCl_2$ (25.0 mg, 0.141 mmol) was added to MeCN (20 mL) and the resulting solution was heated to reflux. A solution of **2a** (45.9 mg, 0.140 mmol) in MeCN (5 mL) was added dropwise. The dark solution was stirred for 20 min at reflux, stirring was stopped, and it was left to sit for 72 h at RT exposed to air. A dark purple solid was collected by filtration (47 mg, 67%). FT-IR (KBr): 3440 (br, m), 3067 (w), 1714 (s), 1605 (m), 1485 (m), 1458 (m), 1447 (m), 1373 (w), 1299 (m), 1241 (m), 1157 (m), 1143 (m), 1104 (m), 1024 (w), 913 (w), 780 (m), 755 (m), 696 (m), 688 (m), 642 (w), 620 (m), 608 (w), 508 (w) cm^{-1}. UV-Vis (MeCN): λ_{max} (nm) (ε, M^{-1} cm^{-1}): 283 (1.4×10^4), 307 (1.4×10^4), 478 (3.5×10^3), 563 (2.4×10^3), 645 (1.7×10^3). Anal. Calc. for $C_{19}H_{14}N_5Cl_2OPd$: C, 45.13; H, 2.79; N, 13.85. Found: C, 44.70; H, 2.56; N, 13.73. MP: >320 °C.

Acknowledgements

We thank the University of Victoria and the Natural Sciences and Engineering Research Council of Canada for support.

Notes and references

1 P. Chaudhuri and K. Wieghardt, *Prog. Inorg. Chem.*, 2001, **50**, 151–216; F. Thomas, *Eur. J. Inorg. Chem.*, 2007, 2379–2404; F. Thomas, in *Stable Radicals: Fundamentals and Applied Aspects of Odd-Electron Compounds*, ed. R. G. Hicks, Wiley, Wiltshire, 2010, pp. 281–316.

2 A. Caneschi, D. Gatteschi and P. Rey, *Prog. Inorg. Chem.*, 1991, **39**, 331–429; D. Luneau and P. Rey, *Coord. Chem. Rev.*, 2005, **249**, 2591–2611; R. A. Sheldon and I. Arends, *J. Mol. Catal. A: Chem.*, 2006, **251**, 200–214; K. E. Vostrikova, *Coord. Chem. Rev.*, 2008, **252**, 1409–1419; C. Train, L. Norel and M. Baumgarten, *Coord. Chem. Rev.*, 2009, **253**, 2342–2351.

3 K. E. Preuss, *Dalton Trans.*, 2007, 2357–2369.

4 R. G. Hicks, *Org. Biomol. Chem.*, 2007, **5**, 1321–1338.

5 T. Buttner, J. Geier, G. Frison, J. Harmer, C. Calle, A. Schweiger, H. Schonberg and H. Grutzmacher, *Science*, 2005, **307**, 235–238; D. Adhikari, S. Mossin, F. Basuli, J. C. Huffman, R. K. Szilagyi, K. Meyer and D. J. Mindiola, *J. Am. Chem. Soc.*, 2008, **130**, 3676–3682; N. P. Mankad, W. E. Antholine, R. K. Szilagyi and J. C. Peters, *J. Am. Chem. Soc.*, 2009, **131**, 3878–3880.

6 *Stable Radicals: Fundamentals and Applied Aspects of Odd-Electron Compounds*, ed. R. G. Hicks, John Wiley & Sons, Wilshire, 2010.

7 R. G. Hicks, in *Stable Radicals: Fundamentals and Applied Aspects of Odd-Electron Compounds*, ed. R. G. Hicks, Wiley, Wiltshire, 2010, pp. 245–280.

8 T. M. Barclay, R. G. Hicks, M. T. Lemaire and L. K. Thompson, *Chem. Commun.*, 2000, 2141–2142; R. G. Hicks, M. T. Lemaire, L. K. Thompson and T. M. Barclay, *J. Am. Chem. Soc.*, 2000, **122**, 8077–8078; T. M. Barclay, R. G. Hicks, M. T. Lemaire and L. K. Thompson, *Inorg. Chem.*, 2001, **40**, 6521–6524; T. M. Barclay, R. G. Hicks, M. T. Lemaire and L. K. Thompson, *Inorg. Chem.*, 2001, **40**, 5581–5584; T. M. Barclay, R. G. Hicks, M. T. Lemaire, L. K. Thompson and Z. Q. Xu, *Chem. Commun.*, 2002, 1688–1689; T. M. Barclay, R. G. Hicks, M. T. Lemaire and L. K. Thompson, *Inorg. Chem.*, 2003, **42**, 2261–2267; R. G. Hicks, B. D. Koivisto and M. T. Lemaire, *Org. Lett.*, 2004, **6**, 1887–1890; M. T. Lemaire, T. M. Barclay, L. K. Thompson and R. G. Hicks, *Inorg. Chim. Acta*, 2006, **359**, 2616–2621.

9 J. B. Gilroy, B. D. Koivisto, R. McDonald, M. J. Ferguson and R. G. Hicks, *J. Mater. Chem.*, 2006, **16**, 2618–2624.
10 S. D. J. McKinnon, J. B. Gilroy, R. McDonald, B. O. Patrick and R. G. Hicks, *J. Mater. Chem.*, 2011, **21**, 1523–1530.
11 D. J. R. Brook, V. Lynch, B. Conklin and M. A. Fox, *J. Am. Chem. Soc.*, 1997, **119**, 5155–5162; D. J. R. Brook, S. Fornell, B. Noll, G. T. Yee and T. H. Koch, *J. Chem. Soc., Dalton Trans.*, 2000, 2019–2022; D. J. R. Brook, S. Fornell, J. E. Stevens, B. Noll, T. H. Koch and W. Eisfeld, *Inorg. Chem.*, 2000, **39**, 562–567; J. E. Stevens, D. J. R. Brook and V. W. Abeyta, *Polyhedron*, 2003, **22**, 2241–2247; D. J. R. Brook, C. J. Richardson, B. C. Haller, M. Hundley and G. T. Yee, *Chem. Commun.*, 2010, **46**, 6590–6592; D. J. R. Brook, G. T. Yee, M. Hundley, D. Rogow, J. Wong and K. Van-Tu, *Inorg. Chem.*, 2010, **49**, 8573–8577.
12 D. J. R. Brook and V. Abeyta, *J. Chem. Soc., Dalton Trans.*, 2002, 4219–4223.
13 L. Norel, F. Pointillart, C. Train, L. M. Chamoreau, K. Boubekeur, Y. Journaux, A. Brieger and D. J. R. Brook, *Inorg. Chem.*, 2008, **47**, 2396–2403; J. B. Rota, L. Norel, C. Train, N. Ben Amor, D. Maynau and V. Robert, *J. Am. Chem. Soc.*, 2008, **130**, 10380–10385; L. Norel, L. M. Chamoreau, Y. Journaux, O. Oms, G. Chastanet and C. Train, *Chem. Commun.*, 2009, 2381–2383; J. B. Rota, C. J. Calzado, C. Train and V. Robert, *J. Chem. Phys.*, 2010, 132.
14 J. B. Gilroy, S. D. J. McKinnon, B. D. Koivisto and R. G. Hicks, *Org. Lett.*, 2007, **9**, 4837–4840.
15 S. D. J. McKinnon, B. O. Patrick, A. B. P. Lever and R. G. Hicks, *Chem. Commun.*, 2010, **46**, 773–775; S. D. J. McKinnon, B. O. Patrick, A. B. P. Lever and R. G. Hicks, *J. Am. Chem. Soc.*, 2011, **133**, 13587–13603.
16 K. J. Anderson, J. B. Gilroy, B. O. Patrick, R. McDonald, M. J. Ferguson and R. G. Hicks, *Inorg. Chim. Acta*, 2011, **374**, 480–488.
17 R. Kuhn and H. Trischmann, *Angew. Chem., Int. Ed. Engl.*, 1963, **2**, 155; R. Kuhn, *Angew. Chem., Int. Ed. Engl.*, 1964, **3**, 762–763.
18 E. K. Y. Chen, S. J. Teertstra, D. Chan-Seng, P. O. Otieno, R. G. Hicks and M. K. Georges, *Macromolecules*, 2007, **40**, 8609–8616.
19 B. Yamada, H. Tanaka, K. Konishi and T. Otsu, *J. Macromol. Sci., Part A: Pure Appl. Chem.*, 1994, **31**, 351–366; B. Yamada, Y. Nobukane and Y. Miura, *Polym. Bull.*, 1998, **41**, 539–544.
20 K. Nakabayashi, Y. Ozaki, M. Kawano and M. Fujita, *Angew. Chem., Int. Ed.*, 2008, **47**, 2046–2048; Y. Ozaki, M. Kawano and M. Fujita, *Chem. Commun.*, 2009, 4245–4247; A. V. Yakovenko, S. V. Kolotilov, O. Cador, S. Golhen, L. Ouahab and V. V. Pavlishchuk, *Eur. J. Inorg. Chem.*, 2009, 2354–2361.
21 F. A. Neugebauer, H. Fischer and C. Krieger, *J. Chem. Soc., Perkin Trans. 2*, 1993, 535–544.
22 R. Milcent, G. Barbier, S. Capelle and J. P. Catteau, *J. Heterocycl. Chem.*, 1994, **31**, 319–324.
23 F. A. Neugebauer, H. Fischer, R. Siegel and C. Krieger, *Chem. Ber./Recl.*, 1983, **116**, 3461–3481.
24 Y. Masuda, M. Kuratsu, S. Suzuki, M. Kozaki, D. Shiomi, K. Sato, T. Takui and K. Okada, *Polyhedron*, 2009, **28**, 1950–1954.
25 K. Mukai, T. Hatanaka, N. Senba, T. Nakayashiki, Y. Misaki, K. Tanaka, K. Ueda, T. Sugimoto and N. Azuma, *Inorg. Chem.*, 2002, **41**, 5066–5074; K. Mukai, N. Senba, T. Hatanaka, H. Minakuchi, K. Ohara, M. Taniguchi, Y. Misaki, Y. Hosokoshi, K. Inoue and N. Azuma, *Inorg. Chem.*, 2004, **43**, 566–576; K. Suzuki, M. M. Matsushita, H. Hayashi, N. Koga and T. Sugawara, *New J. Chem.*, 2008, **32**, 2201–2208.
26 E. C. Constable, R. P. G. Henney, T. A. Leese and D. A. Tocher, *J. Chem. Soc., Chem. Commun.*, 1990, 513–515; F. Neve, M. Ghedini and A. Crispini, *Chem. Commun.*, 1996, 2463–2464; S. W. Lai, T. C. Cheung, M. C. W. Chan, K. K. Cheung, S. M. Peng and C. M. Che, *Inorg. Chem.*, 2000, **39**, 255–262; F. Neve, A. Crispini, C. Di Pietro and S. Campagna, *Organometallics*, 2002, **21**, 3511–3518; Y. J. Kim, X. H. Chang, J. T. Han, M. S. Lim and S. W. Lee, *Dalton Trans.*, 2004, 3699–3708; C. M. A. Ollagnier, S. D. Perera, C. M. Fitchett and S. M. Draper, *Dalton Trans.*, 2008, 283–290; A. Zucca, G. L. Petretto, M. L. Cabras, S. Stoccoro, M. A. Cinellu, M. Manassero and G. Minghetti, *J. Organomet. Chem.*, 2009, **694**, 3753–3761; E. W. Ainscough, H. R. Allcock, A. M. Brodie, K. C. Gordon, M. D. Hindenlang, R. Horvath and C. A. Otter, *Eur. J. Inorg. Chem.*, 2011, 3691–3704.
27 F. A. Neugebauer, H. Brunner and K. H. Hausser, *Tetrahedron*, 1971, **27**, 3623–3628.
28 R. T. Boere and K. H. Moock, *J. Am. Chem. Soc.*, 1995, **117**, 4755–4760; X. Chi, M. E. Itkis, B. O. Patrick, T. M. Barclay, R. W. Reed, R. T. Oakley, A. W. Cordes and R. C. Haddon, *J. Am. Chem. Soc.*, 1999, **121**, 10395–10402; L. Beer, J. L. Brusso, A. W. Cordes, R. C. Haddon, M. E. Itkis, K. Kirschbaum, D. S. MacGregor, R. T. Oakley, A. A. Pinkerton and R. W. Reed, *J. Am. Chem. Soc.*, 2002, **124**, 9498–9509.
29 P. Kaszynski, *J. Phys. Chem. A*, 2001, **105**, 7626–7633.
30 B. Mondal, V. G. Puranik and G. K. Lahiri, *Inorg. Chem.*, 2002, **41**, 5831–5836.

